Mechanism of drug release from silica-gelatin aerogel – relationship between matrix structure and release kinetics

Péter Veres[a], Mónika Kéri[b], István Bányai[b], István Lázár[a], István Fábián[a], Concepción Domingo[c] and József Kalmár[d]*

[a] Department of Inorganic and Analytical Chemistry, University of Debrecen, Egyetem tér 1, H-4032 Hungary

[b] Department of Physical Chemistry, University of Debrecen, Egyetem tér 1, H-4032 Hungary

[c] Institut de Ciència de Materials de Barcelona (CSIC), Campus de la UAB, 08193 Bellaterra, Spain

[d] MTA-DE Homogeneous Catalysis and Reaction Mechanisms Research Group, Egyetem tér 1, H-4032 Hungary

* Corresponding author: e-mail: kalmar.jozsef@science.unideb.hu, tel: +36-52-512-900/22373

Abstract. A comprehensive study of a silica-gelatin aerogel of 3 wt.% gelatin content with applications in drug delivery has been carried out. The release of both ibuprofen (IBU) and ketoprofen (KET) is one order of magnitude faster from loaded silica-gelatin aerogel than from pure silica aerogel, in spite of the structural similarities of the two matrices. The main goal of the study was to understand the mechanistic background of the striking difference between the delivery properties of the two structurally similar porous materials. Hydrated and dispersed silica-gelatin aerogel has been characterized by NMR cryoporometry, diffusiometry and relaxometry. When silica aerogel disintegrates in water its pore structure remains intact. Conversely, dispersed silica-gelatin aerogel develops a strong hydration sphere, which reshapes the pore walls and deforms its pore structure. In view of the structural characteristics of the aerogel delivery matrices, high resolution drug release curves were analyzed in-depth. By compiling all relevant kinetic and structural information, we concluded that the strong hydration of the silica-gelatin skeleton facilitates the rapid desorption and dissolution of drugs from the loaded aerogel. Delivery systems based on pure silica lack this driving force.

Keywords. aerogel structure, drug release, kinetics, NMR spectroscopy

1. INTORDUCTION

Aerogels have excellent adsorption properties due to their open mesoporous structure and huge specific surface area. [1-3] Silica based aerogels [4] are promising platforms for drug delivery applications, mainly due to their high loading capacity, the enhancement of drug stability after adsorption and, in specific cases, the increased bioavailability of active ingredients. [5] These properties, combined with their tunable composition and surface characteristics made them excellent candidates for the pharmaceutical industry as drug delivery systems (DDS). The feasibility of using pure silica aerogels with different structures as DDS has been thoroughly investigated. [2, 6-9] One of the main drawbacks of these systems is that the release of drugs from the silica matrix is hard to fine-tune. Furthermore, the release does not have a well-defined rate, often starting with an uncontrolled burst. [8, 10, 11]

For these reasons, the scope of the development of aerogel based DDS turned towards new organic or hybrid aerogels, involving biological macromolecules or biopolymers (peptides or polysaccharides). Numerous research groups published innovative ideas on the synthesis of aerogels with different composition and structure with high drug encapsulation efficiency and capability of protecting the active agent from various types of environmental effects (humidity, UV radiation). [12-17]

For biopolymer aerogels, the composition, pore structure and hydrophobicity predetermines several fundamental properties in drug delivery applications: 1) the phase (crystalline or amorphous) of the loaded drug, 2) the dispersion of the solid drug in the aerogel matrix, and 3) the accessibility of the solid drug for the solvent during release. These properties determine together the release profile (desorption kinetics) of the drugs from the delivery system. In spite of the numerous publications in the field, no systematic study has been conducted to investigate the relationship between the structure (and composition) of the aerogel and the observed release profile.

In order to understand the drug loading and release (adsorption/desorption) behavior of aerogels, their interaction with different solvents have to be thoroughly studied. Recently, NMR cryoporometry and NMR diffusiometry have been successfully implemented in our laboratories to describe the structure of different porous materials dispersed in liquids, and to gain insights into their interactions with solvent molecules. NMR cryoporometry can be applied to describe the surface properties and wetting characteristics of porous materials of different structures by changing the polarity of the applied test liquid (e.g. water or

cyclohexane). [18] The swelling process of an aerogel and the deformation of the gel structure can be also followed by titrating the solid sample with water [19] or with cyclohexane. The self-diffusion of molecules can be determined with the PGSE (Pulse Field Gradient Stimulated Echo) NMR experiment. The apparent self-diffusion coefficient of small molecules confined in porous materials is often smaller than in the bulk phase. The molecules reach the pore walls within the observation time of the experiment and bounce off. This restricted diffusion can be followed by changing the observation time. The change of the diffusion coefficient by the observation time gives information on the pore and/or particle size, and also on the permeability of the pore structure. [20, 21]

For fast drug release processes complete in a few minutes, the kinetics cannot be studied with high time-resolution in batch experiments applying sampling and off-line analysis. Here we describe a simple, on-line UV-vis spectrophotometric method to overcome this difficulty. It has been demonstrated that high-quality UV-vis data can be acquired even in the presence of dispersed solids in the photometric cell. [1, 22-24]

In the present study, the main goal was to understand the mechanistic background of the unique drug delivery properties of a silica-gelatin hybrid aerogel by using ibuprofen (IBU) and ketoprofen (KET) as model drugs. The silica-gelatin aerogel with a 3 wt.% gelatin content shows promising loading and release properties, [15] which are markedly different from those of pure silica aerogel. Another goal of the study was to understand the mechanistic background of the striking difference between the delivery properties of the two structurally similar porous materials. By simultaneously investigating the pore structure, surface properties and hydration behavior of silica-gelatin aerogel, factors altering the loading and release characteristics can be ascertained. Hence, the structural study was accompanied by a detailed investigation of the release kinetics of the model drugs from the silica-gelatin matrix.

2. EXPERIMENTAL

2.1. Materials

Tetramethylorthosilicate (TMOS) and household gelatin were obtained from Fluka and Dr. Oetker, respectively. Methanol, acetone and $(NH_4)_2CO_3$ were purchased from Fluka. Ibuprofen [2-(4-(2-methyl-propyl)phenyl) propanoic acid] and ketoprofen [2-(3-benzoyl-phenyl propanoic acid] were purchased from Sigma Aldrich. Supercritical CO_2 was produced from 99.95% pure gas (Carburos Metalicos SA). All aqueous solutions were prepared with Milli-Q water (Millipore). Other chemicals (HCl, NaOH, NaH_2PO_4, cyclo-hexane and hexane) were ACS reagent grade (Sigma-Aldrich).

2.2. Aerogel preparation and loading

Silica-gelatin hybrid aerogel was synthesized via a sol-gel process, as reported previously. [15] To produce the composite polymer backbone, a co-gelation method was applied. First, 0.10 g of gelatin and 70.0 mg of $(NH_4)_2CO_3$ were dissolved in 20.0 g of hot water. After cooling to room temperature, a second solution containing 3.30 g of tetramethyl orthosilicate (TMOS) and 5.55 g of MeOH was added to the first one under vigorous stirring. Methanol, and thus TMOS were used instead of the most commonly used ethanol and TEOS, because TEOS hydrolyses slower when applying a basic catalyst and solubility problems can arise in sols with high water content. After mixing the 2 precursor solutions, a costume developed protocol was implemented to produce aerogel monoliths. [25] The mixture was poured in a cylindrical plastic mold for gelation. After 24 h, the alcogel was removed from the mold and placed into a perforated aluminum container for multistep solvent exchange. First, the sample was soaked in methanol for 24 h to remove water. Next, methanol was replaced by acetone in four 24 h soaking steps, and acetone was replaced 2 more times after 24 h soaking. Finally, acetone was extracted with liquid CO_2 at 5.4 MPa (room temperature), then the gel was dried with supercritical CO_2 at 14 MPa and 80 ºC. The resulting silica-gelatin aerogel contains 3 wt.% gelatin according to thermogravimetry. [15] Gelatin is incorporated in the silica backbone and does not leech in water during a week-long soaking.

Pure silica aerogel was prepared by the same process, as detailed above, but without the addition of gelatin to the aqueous $(NH_4)_2CO_3$ solution. This silica aerogel was used as a control for structural comparison with silica-gelatin.

Silica-gelatin aerogel was loaded with ibuprofen (IBU) and ketoprofen (KET) from a supercritical CO_2 solution as described previously. [15] Aerogel powder was wrapped in filter paper and placed into a 100 mL high pressure chamber together with an excess amount of the drug. After the reactor was heated up to 45 °C, liquid CO_2 was pumped in until the pressure reached 20 MPa. After 6 h of stirring under these conditions, the reactor was depressurized with a rate between 0.2-0.3 MPa/min.

2.3. Aerogel characterization

Scanning electron microscopic (SEM) images were recorded on a Hitachi S-4300 instrument (Hitachi Ltd., Tokyo, Japan). Grinded aerogle was immobilized on carbon tape and covered by a sputtered gold conductive layer. Typically, 10 – 15 kV accelerating voltage was used.

Specific surface area, pore size distribution and pore volume of the aerogel was measured by low-temperature N_2 adsorption/desorption porosimetry (Quantachrome Nova 2000e) after degassing the samples at 80 °C for 24 h. Specific surface area and pore size distribution were calculated using the multipoint BET and BJH methods, respectively.

The FT-IR spectra of silica-gelatin aerogel, crystalline IBU and KET, and drug loaded aerogels were recorded using a Perkin-Elmer Spectrum One spectrophotometer after pelleting into KBr.

The particle size distribution of ground silica-gelatin aerogel particles suspended in either water or in hexane was measured in a laser diffraction particle size analyzer (Malvern Mastersizer 2000, Malvern Instruments Ltd., UK). Angular scattering intensity data were evaluated by the instrument controlling software using the Mie theory of light scattering. A representative refraction index of 1.006 was used in the calculations for the aerogel. Particle size is reported in this work as volume equivalent sphere diameter.

2.4. NMR measurements

For NMR measurements, dry (as prepared), ground silica-gelatin aerogel was introduced into glass or Teflon NMR tubes and wetted with either Millipore water, hexane (puriss), or with cyclohexane (puriss). The mass of the aerogel and the liquid added was carefully measured in each experiment. The samples were degassed by sonication.

^{1}H-NMR spin echo and PGSE (Pulse Field Gradient Stimulated Echo) experiments were performed with a Bruker Avance II 400 NMR spectrometer using standard pulse programs provided with the spectrometer. MestreNova 8.1 software was used for FID post processing.

Diffusiometry. Silica-gelatin aerogel suspensions in water and in hexane were studied. The self-diffusion coefficients of water and hexane were measured by standard PGSE protocols. [26] The self-diffusion of the liquids were determined under 2 different conditions. First, having the pores of the aerogel only partially filled with one of the liquids, and second having the pores totally filled with either water or hexane with additional bulk liquid present in the suspension. The technical details of the measurements and data evaluation are mentioned in a previous work [1] and detailed in the Supporting Information.

Cryoporometry. The pore size distribution of suspended silica-gelatin aerogel micronized particles was studied by using 2 different probe liquids, either water or cyclohexane. The aerogel slurries were frozen at −15 °C in a Teflon NMR tube. The probe head was also cooled to this temperature before measurements using a built-in regulator operating with air flowing through a Bruker BSCU-05 cooling unit. The temperature was calibrated using glycol and methanol. [27] The samples were melted by elevating the temperature above the bulk melting points in 0.2 °C steps. From the highest temperature, the samples were cooled to −14 °C in 0.2 °C steps and freezing was monitored. In most freezing experiments, the samples were not completely melted before a freezing cycle was started, necessary to avoid overcooling. The melting and freezing point depressions of liquids in confined spaces and the melting-freezing hysteresis is given by the modified Gibbs–Thomson equations. [28-30] Further details on data evaluation are given in a previous work [1] and in the Supporting Information.

Relaxometry. T_1 relaxation times of the dispersing liquid in aerogel suspensions were measured by inversion recovery. The delay between the 180 and 90 degree power pulse was changed from 0.001 to 5 or 15 s for water or hexane, respectively, in 14 to 24 steps. For T_2 measurement, the CPMG sequence was used. The echo time was set to 0.5 ms and the number of echoes increased from 2 to 50 or to 100. T_1 and T_2 relaxation times were calculated from the non-linear exponential fitting of the measured values by the MestreNova and Origin softwares. The standard deviations of the estimated parameters were also determined in the fitting procedure.

2.5. Drug release experiments

The drug content of loaded IBU and KET loaded samples was measured by soaking some aerogel in a given volume of MeOH, and determining the concentration of dissolved drug by spectrophotometry. Drug release was followed in HCl and phosphate buffered saline solution (PBS), as described previously. [15]

The release of IBU and KET from silica-gelatin aerogel are fast both in HCl and PBS buffer. [15] In order to follow the fast release of the drugs with sufficiently high time-resolution, a new experimental method was developed. Dry, loaded aerogel was milled, and sieved to uniform size (< 125 μm) in order to avoid any size-related effects. A given amount from the loaded aerogel powder was weighted with 0.01 mg precision into a carefully dried spectrophotometric cuvette. The cuvette was placed into the cell of a custom built fiber optic UV-vis spectrophotometer equipped with a fast CCD detector (Avantes) [22] and thermostated at 37.0 °C. On-line detection was started, and 3.0 mL pre-heated release medium (pH 2.0 HCl solution or pH 7.4 PBS) was injected into the cuvette. During this process and under the whole length of the release experiment the suspension was stirred by a 2 × 8 mm PTFE coated magnetic stirbar at 300 rpm. The detector was typically operated with 30 ms integration time and 20 subsequent spectra were averaged. Absorbance change was followed in the 200 – 800 nm wavelength range with 1.0 nm steps for at least 1000 s with a minimum time resolution of 1.0 s. As the drug was released from the aerogel, the characteristic absorbance signal of either IBU or KET was detected in the suspension.

It should be noted, that the aerogel suspension scatters the detection light of the spectrophotometer. However, the apparent absorbance of the suspended aerogel quantitatively adds up with the absorbance of the dissolved substances and do not change the molar absorbances of these analytes, as shown previously. [1, 22] The apparent absorbance of the aerogel was taken into correction by subtracting it from each recorded spectrum using the "dual-wavelength method" developed by Liu and Zhu. [23, 24] First, the spectrum of the aerogel has to be measured under the applied conditions. Second, a reference wavelength range has to be chosen where the dissolved analytes have zero absorbance. The spectrum of the aerogel suspension is reconstructed from the reference absorbances by using the known apparent molar absorbances of the suspension. Finally, the spectrum of the suspension is subtracted from the recorded UV-vis spectrum in the whole wavelength range. This calculation should be done in each experiment at every time point. The corrected, time-

resolved UV-vis spectral series correspond exclusively to the dissolved analytes, giving the drug release curve.

The release experiments were conducted in the concentration range between 0.20 and 0.57 mg/mL loaded aerogel in the dissolution medium. This translates to final concentrations of 0.048 – 0.14 mg/mL and 0.028 – 0.080 mg/mL of IBU and KET, respectively.

3. RESULTS AND DISCUSSION

3.1. Structural characteristics

First, the structural characteristics and wetting properties of silica and silica-gelatin aerogels are compared from the drug delivery point of view. The studied aerogel samples were prepared by the same synthetic process, thus, the differences between the two aerogels can be exclusively attributed to the incorporation of gelatin into the silica backbone.

3.1.1. Scanning electron microscopy

SEM images of silica and silica-gelatin aerogels in 25k× magnification are shown in Figure 1. Both aerogel backbones are built from spherical blocks. The determination of the diameters of the globules is difficult, because they overlap on the image. A rough estimation gives the globule size of both aerogels to be between 75 and 100 nm. The majority of pores are in the mesopores range, although some macropores can be also seen in the images. No significant morphological differences are revealed between the two aerogels.

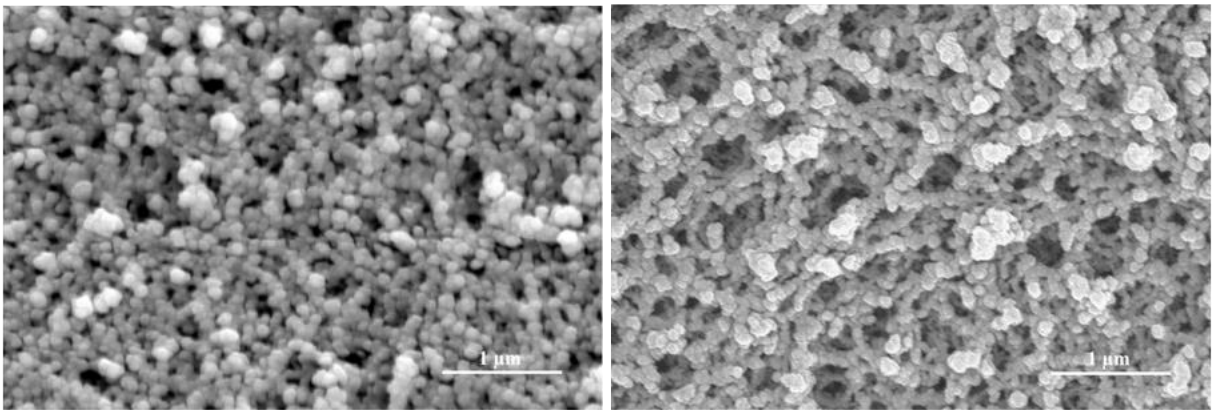

Figure 1. SEM images of silica aerogel (left) and silica-gelatin-aerogel (right).

3.1.2. N_2 adsorption/desorption porosimetry

The N_2 adsorption and desorption isotherms of dry silica-gelatin aerogel and silica aerogel are shown in Figure S1 in the Supporting Information. Type IV hysteresis curves, characteristic for mesoporous materials, were observed for both samples. The steep rise of the isotherms in the vicinity of $p/p_0 = 1$ value indicates the presence of macropores. The specific surface area of silica aerogel is 768 m^2/g and that of the composite is 644 m^2/g determined by multipoint BET. The *C* constants are 70 and 73 for the silica and for the composite, respectively, suggesting highly hydrophilic surfaces in both cases. Total pore volume of silica and silica-gelatin aerogels are 6.00 and 4.95 cm^3/g, respectively. Micropore volumes of both aerogels were near zero as determined by the "t-plot" method. Macropore contributions in the total pore volumes were 1.95 and 0.74 cm^3/g, respectively. This indicates quite well that the mesopore volume of both aerogels are nearly identical. The pore size distributions for the two materials calculated by the BJH method from the desorption curves are shown in Figure 2. The maximum of the distribution curve is shifted from *r*(pore) = 30 – 40 nm for silica to *r*(pore) = 25–30 nm for the composite. The incorporation of gelatin induces the shrinking of the pores, which is also expressed in a decrease of the specific surface area.

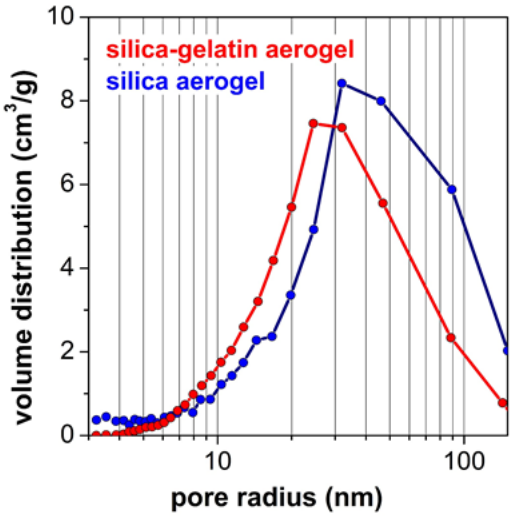

Figure 2. Pore size distribution of dry silica and silica-gelatin hybrid aerogels determined by N_2 adsorption/desorption porosimetry. The distributions were calculated from the desorption curves by the BJH method. The corresponding isotherms are shown in Fig. S1 in the Supporting Information.

3.1.3. Particle size distribution in suspension

The rate of drug release from a delivery matrix is highly dependent on the size distribution of the carrier particles dispersed in the release medium. Silica aerogel particles dispersed in deionized water (or in aqueous buffers) evolve in time and the size distribution stabilizes in *ca.* 3 h after dispersing. This phenomenon is described in detail in a previous publication. [1]

In order to compare the size distribution of particles in silica and silica-gelatin aerogel suspensions, dynamic light scattering (DLS) measurements were performed. The size distributions of both aerogels change rapidly after dispersing, which interfere with DLS measurements. Thus, in the first set of experiments only stable suspensions were studied. The calculated, nearly symmetrical log-normal particle size distributions of the dispersed aerogels are shown in Figure 3. Silica-gelatin aerogel particles are smaller (d = 10 – 30 μm) and more uniform in size, while pure silica aerogel particles are larger (d = 20 – 50 μm) and have a wider distribution. In this sense, DLS data do not indicate that incorporating gelatin into the backbone would significantly alter the suspension phase properties of the aerogel.

The particle size distribution of silica-gelatin was also studied in hexane – EtOH (9:1). The calculated distribution (Figure S2 in the Supporting Information) displays a uniform, *ca.* 5 μm shift towards higher particle sizes compared to measurements performed in water. This effect can be attributed to the smaller solvate sphere of the particles in hexane.

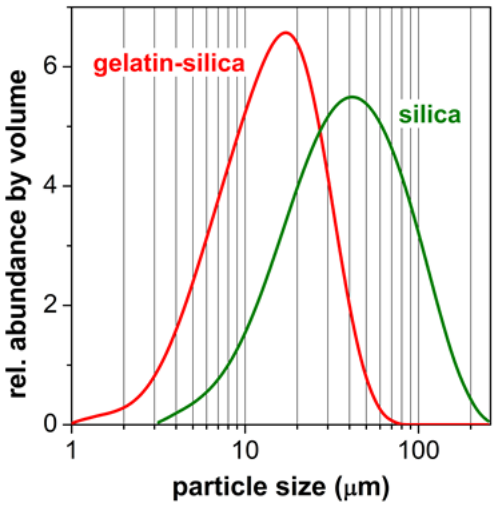

Figure 3. Particle size distribution of silica and silica-gelatin aerogels dispersed in aqueous phosphate buffer. The distributions were calculated from dynamic light scattering (DLS) data. Stable, at least 3 h old suspensions were studied.

In order to directly correlate drug release kinetics with the temporal change in particle size, the size distribution should be followed on the timescale of the release. [10] It was previously shown, that the complete release of IBU and KET from silica and silica-gelatin aerogels takes only a few minutes. [7, 8, 10, 15, 31] Unfortunately, meaningful time-resolved DLS data could not be recorded at this timescale, thus the direct measurement of particle size-distribution during release was not possible. On the other hand, the change of the intensity of scattered light, which also gives indirect information on particle size, was followed with on-line spectrophotometry during drug release experiments. These results are discussed later in Section 3.2.

3.1.4. NMR measurements

Cryoporometry. The pore size distribution of silica aerogel dispersed in water was analyzed by NMR cryoporometry in an earlier study. [1] The general conclusion drawn from cryoporometric data was, that dispersed aerogel particles retain the pore structure of the dry (as prepared) aerogel following the disintegration of the monolith in water. The pore size distribution of the dry silica aerogel measured by N_2 porosimetry and that of the dispersed aerogel measured by cryoporometry are almost identical. [1] During stirring and agitation, the shear forces cause the fragmentation of the large aerogel particles until a suspension with a well-defined particle size distribution is reached, which is confirmed by the DLS results (cf. Fig. 3). However, the pore structure remains intact. This phenomenon was also investigated by small-angle neutron scattering (SANS), and it was shown that the introduction of water into the pores does not affect the structure in the mesoporous range. [32]

The pore structure of silica-gelatin aerogel was probed by two different liquids using NMR cryoporometry. The first liquid was cyclohexane, a nonpolar liquid in which neither gelatin nor silica swell. The melting and freezing curves of silica-gelatin aerogel dispersed in cyclohexane is shown in Figure 4. The position of the melting/freezing hysteresis indicates the presence of mainly spherical pores in the suspension. [30] The reconstructed pore size distribution is shown in Fig. 4. The comparison of the distribution curves in Figs. 2 and 4 indicates that the pore structure of silica-gelatin aerogel is not deformed significantly when the material is dispersed in cyclohexane. This observation is in-line with the expected weak interaction between the hydrophilic silica-gelatin skeleton and cyclohexane.

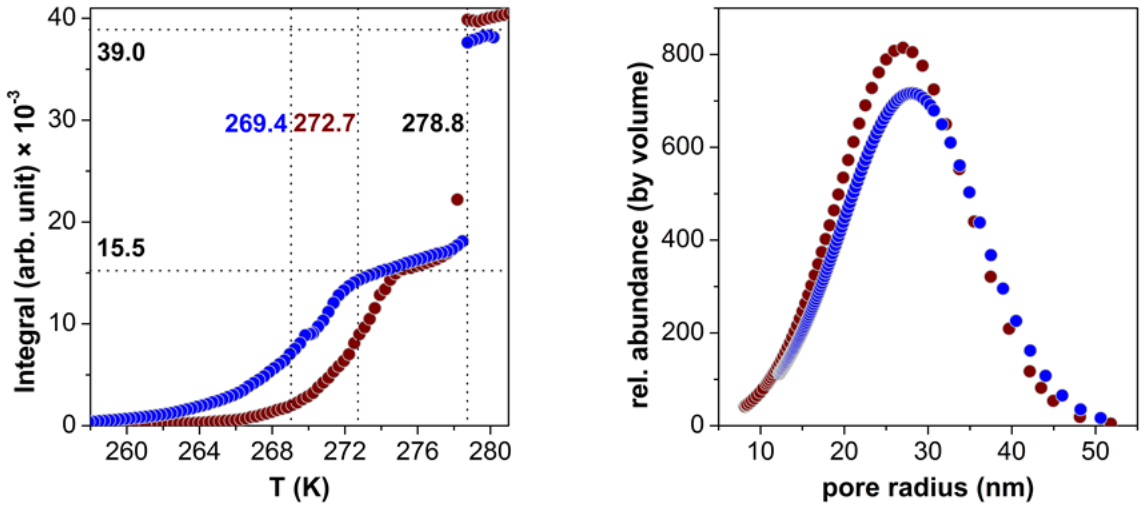

Figure 4. NMR cryoporometry. Left: Melting (red) and freezing (blue) curves of silica-gelatin aerogel dispersed in cyclohexane. The position of the inflection points and the height of the plateaus are given in the plot. Right: Pore size distribution of dispersed silica-gelatin aerogel reconstructed from the left figure assuming spherical pores (red: from the melting curve, blue: from the freezing curve).

The second liquid used for probing silica-gelatin aerogel was water. A suspension of well-defined size distribution was studied (cf. Fig. 3). The cryoporometric melting and freezing curves of the aqueous aerogel suspension show hysteresis, but do not have a well-defined plateau before the melting of bulk water at 273 K (Figure 5). Cryoporometric curves of this type are characteristic for hydrogels, where no solid-walled pores exist and the apparent pore size distribution is extremely wide. [19] When silica-gelatin aerogel is wetted with water stirring and agitation cause the fragmentation of the large aerogel particles until dispersed particles of well-defined sizes are produced. Additionally, silica-gelatin aerogle shows no observable swelling (or shrinking) in water. Still, cryoporometry indicates that its backbone strongly interacts with water. It is rational to assume that the gelatin content in the backbone strongly binds water, and the well-hydrated protein chains deform the whole polymer backbone during their conformational change. The resulting structure resembles a hydrogel in the sense that the well-defined pore structure of the dry aerogel ceases to exist.

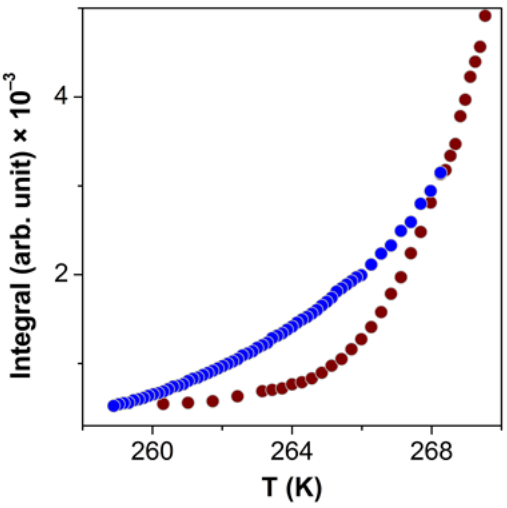

Figure 5. NMR cryoporometry. Melting (red) and freezing (blue) curves of silica-gelatin aerogel dispersed in water. The absence of inflection points and plateaus on the curves indicate a dense hydrogel like structure for the dispersed aerogel particles with no well-defined pore size distribution.

Diffusiometry. In some silica-gelatin aerogel suspensions the self-diffusion of the dispersing liquid was measured by PGSE NMR technique. First, the aerogel was dispersed in ca. twice the amount of hexane necessary to completely fill the pores of the material. Diffusion experiments revealed that the self-diffusion of hexane is restricted in this case. The intensity decay in the diffusion experiment is clearly single exponential (Figure S3 in the Supporting Information) in a wide observation time range from 4 to 120 ms. The value of the observed self-diffusion coefficient is $D_{obs} = (3.30 \pm 0.09)\times10^{-5}$ cm^2/s, while that is 4.15×10^{-5} cm^2/s for bulk hexane. [33] The explanation for the single diffusion domain is related to the fact that hexane molecules in the bulk diffuse freely, but molecules inside the pores are restricted in movement. The two groups of molecules would normally give two diffusion domains, unless they exchange rapidly in the timescale of the diffusion experiment. Rapid exchange between bulk hexane and hexane inside the pores indicates that the structure of the dispersed silica-gelatin aerogel is open and the pores are highly interconnected. Small molecules can enter and exit the pore network without restriction in the millisecond timescale. This is not surprising, since cryoporometry showed that dispersion in hexane does not deform the open pore structure of the aerogel.

In the second experiment silica-gelatin aerogel was dispersed in *ca.* twice the amount of water necessary to completely wet and fill the pores of the aerogel. PGSE experiments revealed that the self-diffusion of water is restricted in this aqueous suspension. Surprisingly, we detected only one diffusion domain (single exponential decay, Figure S4 in the Supporting

Information) in the whole timescale of the diffusion experiments (4 – 120 ms). The observed self-diffusion coefficient is D_{obs} = (1.5 ± 0.1)×10^{-5} cm^2/s, while this is 2.3 × 10^{-5} cm^2/s for bulk water. [34] By applying the same reasoning as in the case of hexane, the single diffusion domain indicates that hydrated and dispersed aerogel particles are still highly permeable for water. Cryoporometry revealed that silica-gelatin aerogel particles develop a hydrogel like character in water. Now, the results of diffusiometry complete this information by suggesting that in spite of the high extent of hydration and deformation of the aerogel, the pore structure remains interconnected and highly permeable.

In order to gain more information on the interaction of silica-gelatin aerogel with water, additional PGSE experiments were performed with wet aerogel samples, containing only *ca.* 70% of the amount of water necessary to completely fill the pores of the aerogel. In this case, at short observation times (< 40 ms) the value of the observed self-diffusion coefficient decreases by increasing observation time. At longer observation times two separate diffusion domains (i.e. double exponential decays) were observed (Figure S5 in the Supporting Information). The dependence of the diffusion coefficients on observation time is shown in Figure 6. We propose, that the slower diffusion domain is characteristic for water molecules in the close hydration sphere of the silica-gelatin polymer backbone. Water molecules outside the hydration sphere, diffusing in the pores belong to the faster diffusion domain. The fact that the two domains are not separated at short observation times indicates that water in the close hydration sphere cannot travel large enough distances to feel spatial hindrance in short time. [20, 21] The size of the restricting space can be approximated by using the methodology of Cho *et.al.*, [21] as D_{obs} is inversely proportional to the observation time in this region. By using the Einstein equation, we found that water molecules in the hydration sphere can travel *ca.* 26 μm freely, which is the approximate size of a dispersed aerogel particle. Evidently, when the silica-gelatin aerogel particles are only wet and no bulk water is present, water molecules in the close hydration sphere of the polymer backbone are restricted from moving from one particle to another. This is another piece of evidence for the strong hydration of silica-gelatin aerogel.

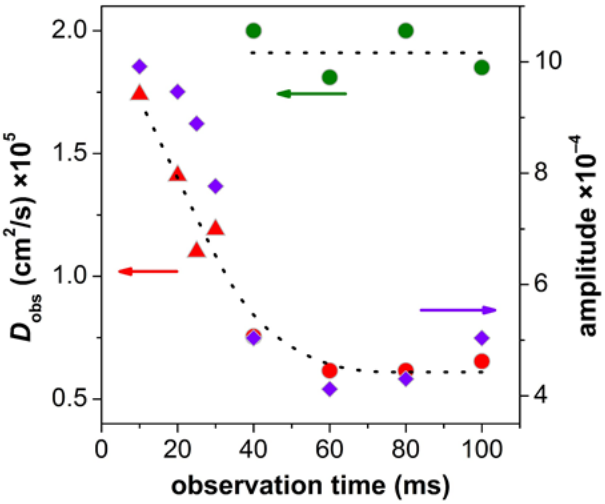

Figure 6. NMR diffusiometry. The self-diffusion coefficient (D_{obs}) of water measured in a wet silica-gelatin aerogel sample. Approximately 70% of the total pore volume of the aerogel is filled with water. Two diffusion domains were detected at observation times ≥ 40 ms. The diffusion coefficient of the faster domain is given with green, that of the slower domain is given with red. The amplitude characterizing the slower domain is also given with violet. The measured D_{obs} of the slower domain is increasing by decreasing observation time. The detailed explanation is given in the text of the article (Section 3.1.4. Diffusiometry). Dashed lines are only for guiding the eye.

Relaxometry. The T_1 and T_2 relaxation times of the dispersing liquids were measured in suspensions made with hexane or with water. Two pairs of experiments were performed. The relaxation times were measured when the pores of the aerogel were partially filled with either water or hexane, and also when the pores were completely filled and bulk liquid was present in the suspension. The relaxation times together with the standard deviations of parameter estimation are shown in Table 1.

In the case of both liquids, two different T_2 relaxation times were observed independently from the amount of liquid used for dispersion. The smaller T_2 can be attributed to solvent molecules in close interaction with the surface of the aerogel (adsorbed), while the higher values can be attributed to the average relaxation of molecules inside the pores and in the bulk. By increasing the amount of the dispersing liquids, the T_2 relaxation times increase, as the relative amount of solvent molecules in close interaction with the surface decrease. According to the cryoporometric experiments the interaction of water with silica-gelatin is much stronger than in the case of hexane, resulting in faster transverse relaxation (T_2) relaxation due to the longer rotation correlation time (τ_c) of water molecules in the hydrated matrix.

Table 1. NMR relaxation times of liquids used for dispersing silica-gelatin aerogel. In the first set of experiments the aerogel was only wetted with the probe liquids and no bulk phase was present. In the second set of experiments *ca.* twice the amount of liquid was used as in the previous set. Two T_2 relaxation processes were observed in each sample. The error values are the standard deviations of the estimated parameters determined in the non-linear fitting process.

Solvent	Saturation of pores with liquid	T_1 (s)	T_{2a} (s)	T_{2b} (s)
water	ca. 70%	1.84 ± 0.02	$(3.2 \pm 0.1) \times 10^{-3}$	$(9.9 \pm 0.3) \times 10^{-3}$
	100%, bulk liquid present	0.91 ± 0.01	$(3.9 \pm 0.8) \times 10^{-3}$	$(1.8 \pm 0.1) \times 10^{-2}$
hexane	ca. 70%	2.97 ± 0.09	$(4.7 \pm 0.2) \times 10^{-3}$	$(2.1 \pm 0.1) \times 10^{-2}$
	100%, bulk liquid present	3.88 ± 0.05	$(1.0 \pm 0.2) \times 10^{-2}$	$(1.2 \pm 0.1) \times 10^{-1}$

While T_2 relaxation time decreases monotonously with increasing rotation correlation time, T_1 relaxation time shows a minimum curve. [35] Water molecules in the strongly hydrated aqueous sample are in a higher rotation correlation time range, where T_1 decreases with τ_c. By increasing the amount of water in the sample and introducing some bulk liquid, the movement of water molecules become less hindered. The rotation correlation time of water molecules decrease and T_1 decreases, as seen in Table 1. In the case of hexane, the aerogel is not well-solvated and the solvent molecules can rotate faster. Thus, hexane molecules are in a smaller τ_c region where the T_1 relaxation time is inversely proportional with τ_c. This results in increasing T_1 with the increasing amount of the dispersing liquid (Table 1).

3.1.5. Silica and silica-gelatin aerogels: similarities and differences

Nitrogen porosimetry and SEM (Sections 3.1.1 and 3.1.2) showed that there is no remarkable difference between the structures of dry (as prepared) silica-gelatin and silica aerogels, besides that the pores of the former are somewhat smaller in the mesopore range. DLS measurements (Section 3.1.3) confirmed, that both silica and silica-gelatin aerogels degrade to 10 – 30 μm particles in water. The stable suspension of silica-gelatin contains smaller particles than that of silica. Silica and silica-gelatin aerogels were probed by the method of NMR cryoporometry using water as the test liquid (Section 3.1.4). These measurements proved, that silica aerogel retains its pore structure on the level of particles

upon dispersion in water, but the pores of silica-gelatin aerogel become deformed, and the hydrated structure cannot be characterized with a well-defined pore size distribution anymore. In spite of their deformed pore structure, hydrated silica-gelatin aerogel particles are still highly permeable for water, similarly to dispersed silica aerogel particles with intact pores, according to NMR PGSE diffusiometry (Section 3.1.4).

3.2. Drug release experiments

The loading of silica aerogel with non-polar drugs and the release of these substances in different media have been extensively studied previously. [2, 7, 8, 31, 36] According to these sources silica aerogel can take up 20 – 23 wt.% ketoprofen (KET) and more than 40 wt.% ibuprofen (IBU) from supercritical CO_2 via adsorptive deposition. We have shown that silica-gelatin aerogel with 3 wt.% gelatin content can take up 24 wt.% IBU and 14 wt.% KET. [15] The IR spectra of loaded silica-gelatin aerogels are given in the Supporting Information. The lower loading compared to silica can be attributed to the decrease of the specific surface area of the aerogel due to the incorporation of gelatin. It should be noted that the surface specific loading of silica-gelatin aerogel is higher than that of pure silica, which indicates the somewhat higher affinity of the drugs towards the former. [15] It was also shown by XRD in the case of both silica and silica-gelatin aerogels, that the drugs condense as non-crystalline solids inside the pores. [8, 15]

The release of IBU and KET from loaded silica and silica-gelatin aerogels have not been previously compared, in spite of the obvious similarities of the delivery matrices. The release of KET from silica aerogel always starts with a rapid (burst) release, in which 20 – 40% of the total loading dissolves in 5 min, while complete release is reached in a subsequent slower step in 50 – 100 min. [2, 5, 7, 31, 36] Interestingly, the complete dissolution of both KET and IBU from silica-gelatin aerogel are almost ten-times faster processes, complete in only a few hundred seconds. [15]

In order to gain sufficient amount of kinetic information on the rapid release of IBU and KET from silica-gelatin aerogel, a special, on-line spectrophotometric technique was developed. The details are described in the Experimental section, and in previous papers. [1, 22] Owing to the 1.0 s time resolution of the method, high quality kinetic curves could be recorded even in the case of the silica-gelatin rapid delivery system. It is also important to note that in the current study milled and sieved aerogle particles were used to avoid any size-

related effects during dissolution. The release profiles in pH 2.0 HCl and in 10 mM PBS media are shown in Figure 7. These high quality profiles can be analyzed quantitatively, and the intimate mechanism of release can be elucidate with model fitting, and compared to the structural properties of the delivery matrix.

Therefore, the results presented here are considered richer in information and more reliable than those obtained in our preliminary studies and published earlier. [15] The release kinetics were re-evaluated in the light of the new results in order to gain a deeper understanding on the mechanism of drug dissolution and on the various factors governing it.

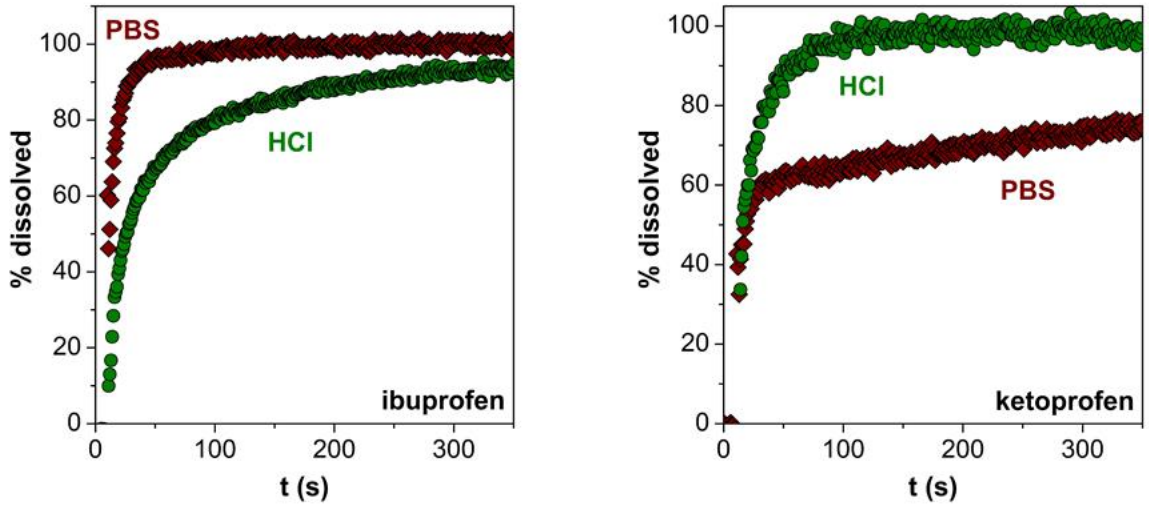

Figure 7. Drug release experiments. The dissolution of ibuprofen (left) and ketoprofen (right) from loaded silica-gelatin aerogel. Two sets of experiments were performed, one in pH 2.0 HCl and another in 10 mM PBS (pH 7.4). Additional curves are shown in Figure S8 in the Supporting Information. The detailed kinetic analysis of the release profiles are given in the main text of the paper (Sections 3.2.1. and 3.2.2). Mass of loaded aerogel: 1.50 mg, volume of release medium: 3.0 mL, T = 37.0 °C, 300 rpm stirring.

3.2.1. Release kinetics in PBS

The release of IBU is complete in 100 s in PBS. In one set of parallel experiments the amount of loaded aerogel in the dissolution cell was modified keeping the volume of PBS constant (Figure S8 in the Supporting Information). In these runs, the absolute amount of dissolved IBU increases with increasing amount of loaded aerogel. However, the relative amount of dissolved IBU at a given time, i.e. the release profile, does not change with changing aerogel concentration, as seen in Fig. S8. This observation makes two facts clear: first, the solubility of IBU does not limit its release, and second, the relative rate of

dissolution is invariant to both the concentration of loaded aerogel and the concentration of dissolved IBU.

Aerogels are considered eroding delivery systems, [5, 10, 37] meaning that the kinetics of release is primarily governed by the rate of matrix erosion and only secondarily by the limited diffusion of drug molecules from the pores. The Hopfenberg model is a semi-empirical model which can be advantageously used to describe the kinetics of drug release from eroding matrices. [37, 38] Non-linear fitting of the release curves shown in Fig. 7 was performed accordingly. The best results were obtained by using the Hopfenberg model valid for spherical (n = 3) degrading systems, as shown in the Supporting Information (Figure S9). Nevertheless, the shapes of the measured and the fitted curves deviate systematically. Additionally, the first 60% of the release curves were fitted to widely used empirical release models (first order, Higuchi, Peppas, Hixon-Crowell), but none of these models are able describe the release of IBU in PBS from silica-gelatin aerogel. Thus, it is evident, that the rate of drug release is controlled by matrix specific physico-chemical processes, rather than general transport processes. Possible factors that might control the release kinetics are the adsorption of the drug, and the erosion, deformation and hydration of the silica-gelatin backbone.

The kinetics of drug release is affected by the strength (i.e., the energy) of the specific interaction between the drug molecules and the pore walls. [39, 40] If the interaction is strong, the effective diffusion of the drug molecules are slowed. In this case, the release kinetics is at least partially controlled by the aforementioned specific interaction. [39, 40] In our previous work, it was shown that the affinity of IBU is somewhat higher towards the surface of silica-gelatin than towards pure silica. [15] Thus, a stronger surface interaction is expected between IBU and silica-gelatin, then between IBU and silica. In spite of the stronger interaction, the release rate is much faster from the silica-gelatin matrix. A feasible explanation for this phenomenon is that the release rate is not interaction controlled, and the rate determining processes are probably the degradation, deformation and hydration of the aerogel matrix.

The next logical step to understand the mechanism of drug release was the investigation of the kinetics of the erosion of the silica-gelatin aerogel matrix in water. Unfortunately, as mentioned in Section 3.1.3, we could not use time-resolved DLS to follow the degradation of the dispersed aerogel during drug release. However, we could follow the light scattering of the suspension on-line by UV-vis spectrophotometry at wavelengths where dissolved IBU does not absorb. The detailed description of these experiments are given in the Supporting Information, and results are shown in Figure S10. It was found that the light

scattering of the suspension is practically constant in the timescale of release, meaning that the size distribution of the dispersed aerogel particles does not change. This indicates, that the observed limited erosion of the silica-gelatin particles can control only the initial, burst phase of the release kinetics. [2, 5, 8, 40] Evidently, the later phase of the release kinetics is controlled by other processes, most probably the deformation and the hydration of the pore structure.

By summarizing all the above experimental results and theoretical considerations, it seems rationale that the key factor which forces the rapid desorption and dissolution of IBU from the silica-gelatin aerogel is the hydration of the matrix. Furthermore, the changing, opening pore structure can be also advantageous in facilitating the rapid release of the model drug. Another important conclusion is that the only major difference between the silica and silica-gelatin delivery systems is the strong hydration of the latter, which property radically changes the rate of drug release.

On the longer time-scale, however, the hydration of the silica-gelatin aerogel matrix is expected to hinder the diffusion of drug molecules, because the effective cross-section of the pores decrease. This scenario can be observed in the case of the release of KET in PBS (Figs. 7 and S8). The release of KET in PBS is significantly slower than the release of IBU in the same medium. In the case of KET, there is enough time for the silica-gelatin matrix to reach complete hydration and develop a hydrogel like structure, which results in retarded release after 100 s.

3.2.2. Release kinetics in HCl

The release of IBU is complete in 400 s in HCl. The kinetic curves have similar shapes in HCl and in PBS, meaning that the rate determining process is most probably the same in the two media. Furthermore, the relative rate of drug dissolution is invariant to the IBU concentration in HCl also (Fig. S8). The release curves in Fig. 7 were fitted to the Hopfenberg model, and additionally to empirical release models, as described in the Supporting Information. Fitting was again unsuccessful, indicating that the mechanistic considerations discussed in the case of the PBS medium are valid here as well.

It is interesting to note that the IBU is released much faster in PBS, than in HCl. The reason can be the stronger interaction between the protonated drug and the pore wall in HCl.

The formation of hydrogen bonds between gelatin and IBU is also possible, meaning that the mechanism of drug release can be interaction controlled [39, 40] in HCl.

The shape of the release profiles of KET are markedly different in PBS and in HCl (Figs. 7 and S8). The initial rate is slightly lower in HCl, but the retarded release characteristic in PBS is not present in HCl. A kinetic explanation is proposed as follows. The shape of the release curve is determined by the relative rate of desorption of KET and the formation of the deformed hydrogel structure. When hydrogel formation is much slower than desorption, no retarded effect can be seen. Most probably, hydrogel formation is much faster in PBS than in HCl, thus the relative rate of desorption significantly increases in HCl. This effect can compensate for the decrease of the absolute rate of desorption due to the protonation of KET in HCl.

4. CONCLUSIONS

The dissolution of ibuprofen and ketoprofen from loaded silica-gelatin aerogel is almost one magnitude faster than from pure silica aerogel (both in HCl and in PBS). The main goal of the study was to understand the mechanistic background of the striking difference between the delivery properties of the two structurally similar porous materials. When analyzing the structure of the dry (as prepared) silica and silica-gelatin aerogels by SEM and N_2 porosimetry, only minor differences were found, which cannot account for the markedly different release properties. It was demonstrated via NMR measurements, that in spite of the similarities of the structures of the two aerogels, these materials have distinct hydration properties. While silica disintegrates when placed into water, its pore structure remains intact. Silica-gelatin aerogel, however, develops a strong hydration sphere, which also deforms the backbone and pore walls. Wet silica-gelatin aerogel displays hydrogel like properties, in the sense that it has no longer a well-defined pore structure. We propose that the strong hydration of silica-gelatin is the key factor which significantly accelerates the desorption and dissolution of loaded drugs from the matrix. Delivery systems based on pure silica lack this driving force. The present findings regarding the relationship of the structure and the release properties of composite aerogels can be utilized for the systematic design of future drug-delivery systems.

5. ACKNOWLEDGEMENTS

We are grateful to Lajos Daróczy (University of Debrecen) for the electron microscopy measurements and Attila Sztrik (University of Debrecen) for the laser diffraction measurements. The authors thank the Hungarian Science Foundation (OTKA: NK-105156), the University of Debrecen (RH/751/2015) and the Spanish National Plan of Research (project CTQ2014-56324) for financial support. P. Veres acknowledge the TÁMOP-4.2.4A/2-11/1-2012-0001 and TÁMOP-4.2.4B/2-11/1-2012-0001 projects. The research was supported through the NEW NATIONAL EXCELLENCE PROGRAM of the Ministry of Human Capacities of Hungary.

Electronic Supporting Information (ESI) available:

Detailed experimental for the NMR measurements. Figures referred to in the main text of the article. Porometry, DLS, NMR, IR and kinetic data.

6. REFERENCES

Uncategorized References

[1] J. Kalmár, M. Kéri, Z. Erdei, I. Bányai, I. Lázár, G. Lente, I. Fábián, The pore network and the adsorption characteristics of mesoporous silica aerogel: adsorption kinetics on a timescale of seconds, RSC Adv., 5 (2015) 107237-107246.
[2] I. Smirnova, J. Mamic, W. Arlt, Adsorption of drugs on silica aerogels, Langmuir, 19 (2003) 8521-8525.
[3] S. Standeker, Z. Novak, Z. Knez, Adsorption of toxic organic compounds from water with hydrophobic silica aerogels, J. Colloid Interface Sci., 310 (2007) 362-368.
[4] A. Soleimani Dorcheh, M.H. Abbasi, Silica aerogel; synthesis, properties and characterization, J. Mater. Process. Technol., 199 (2008) 10-26.
[5] Z. Ulker, C. Erkey, An emerging platform for drug delivery: aerogel based systems, J. Control. Release, 177 (2014) 51-63.
[6] A.C. Pierre, G.M. Pajonk, Chemistry of aerogels and their applications, Chem. Rev., 102 (2002) 4243-4265.
[7] I. Smirnova, S. Suttiruengwong, W. Arlt, Feasibility study of hydrophilic and hydrophobic silica aerogels as drug delivery systems, J. Non-Cryst. Solids, 350 (2004) 54-60.
[8] I. Smirnova, S. Suttiruengwong, W. Arlt, Aerogels: Tailor-made Carriers for Immediate and Prolonged Drug Release, KONA, 23 (2005) 86-97.
[9] N. Murillo-Cremaes, A.M. Lopez-Periago, J. Saurina, A. Roig, C. Domingo, Nanostructured silica-based drug delivery vehicles for hydrophobic and moisture sensitive drugs, J. Supercrit. Fluids, 73 (2013) 34-42.

[10] U. Maver, A. Godec, M. Bele, O. Planinsek, M. Gaberscek, S. Srcic, J. Jamnik, Novel hybrid silica xerogels for stabilization and controlled release of drug, Int. J. Pharm., 330 (2007) 164-174.
[11] X. Huang, C.S. Brazel, On the importance and mechanisms of burst release in matrix-controlled drug delivery systems, J. Control. Release, 73 (2001) 121-136.
[12] A. Veronovski, Z. Knez, Z. Novak, Preparation of multi-membrane alginate aerogels used for drug delivery, J. Supercrit. Fluids, 79 (2013) 209-215.
[13] A. Veronovski, G. Tkalec, Z. Knez, Z. Novak, Characterisation of biodegradable pectin aerogels and their potential use as drug carriers, Carbohydr. Polym., 113 (2014) 272-278.
[14] C.A. Garcia-Gonzalez, M. Jin, J. Gerth, C. Alvarez-Lorenzo, I. Smirnova, Polysaccharide-based aerogel microspheres for oral drug delivery, Carbohydr. Polym., 117 (2015) 797-806.
[15] P. Veres, A.M. Lopez-Periago, I. Lazar, J. Saurina, C. Domingo, Hybrid aerogel preparations as drug delivery matrices for low water-solubility drugs, Int. J. Pharm., 496 (2015) 360-370.
[16] H. Maleki, L. Duraes, C.A. Garcia-Gonzalez, P. Del Gaudio, A. Portugal, M. Mahmoudi, Synthesis and biomedical applications of aerogels: Possibilities and challenges, Adv. Colloid Interface Sci., (2016).
[17] J. Stergar, U. Maver, Review of aerogel-based materials in biomedical applications, J. Sol-Gel Sci. Technol., 77 (2016) 738-752.
[18] S.G. Allen, P.C.L. Stephenson, J.H. Strange, Internal surfaces of porous media studied by nuclear magnetic resonance cryoporometry, J. Chem. Phys., 108 (1998) 8195-8198.
[19] M. Keri, C. Peng, X. Shi, I. Banyai, NMR characterization of PAMAM_G5.NH2 entrapped atomic and molecular assemblies, J. Phys. Chem. B, 119 (2015) 3312-3319.
[20] R. Valiullin, V. Skirda, Time dependent self-diffusion coefficient of molecules in porous media, J. Chem. Phys., 114 (2001) 452-458.
[21] C.H. Cho, Y.S. Hong, K. Kang, V.I. Volkov, V. Skirda, C.Y. Lee, C.H. Lee, Water self-diffusion in Chlorella sp. studied by pulse field gradient NMR, Magn. Reson. Imaging, 21 (2003) 1009-1017.
[22] T. Ditroi, J. Kalmar, J.A. Pino-Chamorro, Z. Erdei, G. Lente, I. Fabian, Construction of a multipurpose photochemical reactor with on-line spectrophotometric detection, Photochem. Photobiol. Sci., 15 (2016) 589-594.
[23] H. Liu, J.Y. Zhu, X.S. Chai, In situ, rapid, and temporally resolved measurements of cellulase adsorption onto lignocellulosic substrates by UV-vis spectrophotometry, Langmuir, 27 (2011) 272-278.
[24] Q.Q. Wang, J.Y. Zhu, C.G. Hunt, H.Y. Zhan, Kinetics of adsorption, desorption, and re-adsorption of a commercial endoglucanase in lignocellulosic suspensions, Biotechnol. Bioeng., 109 (2012) 1965-1975.
[25] I. Lázár, I. Fábián, A Continuous Extraction and Pumpless Supercritical CO2 Drying System for Laboratory-Scale Aerogel Production, Gels, 2 (2016) 26.
[26] Y. Cohen, L. Avram, L. Frish, Diffusion NMR spectroscopy in supramolecular and combinatorial chemistry: an old parameter--new insights, Angew. Chem. Int. Ed. Engl., 44 (2005) 520-554.
[27] C. Ammann, P. Meier, A.E. Merbach, A Simple Multi-Nuclear NMR Thermometer, J. Magn. Reson., 46 (1982) 319-321.
[28] J.H. Strange, M. Rahman, E.G. Smith, Characterization of porous solids by NMR, Phys. Rev. Lett., 71 (1993) 3589-3591.
[29] J. Mitchell, J. Webber, J. Strange, Nuclear magnetic resonance cryoporometry, Phys. Rep., 461 (2008) 1-36.
[30] O.V. Petrov, I. Furó, NMR cryoporometry: Principles, applications and potential, Prog. Nucl. Magn. Reson. Spectrosc., 54 (2009) 97-122.
[31] I. Smirnova, S. Suttiruengwong, M. Seiler, W. Arlt, Dissolution Rate Enhancement by Adsorption of Poorly Soluble Drugs on Hydrophilic Silica Aerogels, Pharm. Dev. Technol., 9 (2004) 443-452.
[32] C.I. Merzbacher, J.G. Barker, K.E. Swider, D.R. Rolison, Effect of re-wetting on silica aerogel structure: a SANS study, J. Non-Cryst. Solids, 224 (1998) 92-96.
[33] K.R. Harris, Temperature and Density Dependence of the Self-Diffusion Coefficient of N-Hexane from 223-K to 333-K and up to 400 Mpa, J. Chem. Soc. Farad. Trans., 78 (1982) 2265-2274.

[34] R. Mills, Self-diffusion in normal and heavy water in the range 1-45.deg, J. Phys. Chem., 77 (1973) 685-688.
[35] N. Bloembergen, E.M. Purcell, R.V. Pound, Relaxation Effects in Nuclear Magnetic Resonance Absorption, Phys. Rev., 73 (1948) 679-712.
[36] M. Alnaief, I. Smirnova, Effect of surface functionalization of silica aerogel on their adsorptive and release properties, J. Non-Cryst. Solids, 356 (2010) 1644-1649.
[37] J. Siepmann, F. Siepmann, Mathematical modeling of drug delivery, Int. J. Pharm., 364 (2008) 328-343.
[38] P. Costa, J.M. Sousa Lobo, Modeling and comparison of dissolution profiles, Eur. J. Pharm. Sci., 13 (2001) 123-133.
[39] T. Ukmar, U. Maver, O. Planinsek, A. Pintar, V. Kaucic, A. Godec, M. Gaberscek, Guest-host van der Waals interactions decisively affect the molecular transport in mesoporous media, J. Mater. Chem., 22 (2012) 1112-1120.
[40] T. Ukmar, U. Maver, O. Planinsek, V. Kaucic, M. Gaberscek, A. Godec, Understanding controlled drug release from mesoporous silicates: Theory and experiment, J. Controlled Release, 155 (2011) 409-417.